RESEARCH ARTICLE

Structural and Optical Studies of Quaternary Glass System

V. Sreenivasulu[1], G. Upender[2], V. Chandra Mouli[2], K. Praveena[1,*], M. Prasad[2,*]

The new tellurite glasses with chemical composition $64TeO_2$-15CdO-(20-x) ZnO-xLi_2O-$1V_2O_5$ (x= 0, 5, 10, 15 and 20 mol %) were synthesized by traditional melt quench hardening method. The glass samples showed broad humps of typical amorphous phase in the X- ray diffraction patterns. The physical properties of glass samples such as density (ρ), molar volume (V_m), oxygen packing density (OPD), refractive index (n), molar refractivity (R_m) and metallization parameter (M) were estimated. The Fourier transform infrared spectroscopy (FTIR) studies exhibited that replacement of ZnO by Li_2O forms significantly some basic structural units of TeO_4, TeO_3/TeO_{3+1} and ZnO_4. Differential scanning calorimetry (DSC) was employed to find out the glass transition temperature (T_g) and thermal stability (ΔT). The optical enthrallment studies exhibited that the cut-off wavelength (λ) decreases while optical energy gap (E_{opt}) and Urbach energy (ΔE) values increases with an increase an escalation of Li_2O content. This tellurite glasses possess an important use such as sensor devices, storage of data system and industrial applications etc.

Introduction

Glass is a unique material and it has substantial potentiality in various areas. Generally, glass substances are preferred in day-to-day life, such as doors, windows, and most advanced applications like laser hosts in optical amplifiers, optical modulators, optical displays, optical data storage systems, pressure sensors in different scientific laboratories, medical fields and military uses. In the current scenario high transparency and strength of durability are prominent characters of glasses. Arsenate, phosphate, silicate, germinate and borate are different varieties of glass materials. Because of transparency and simple performance, the glass substance could be used for protection purpose [**1-5**]. The heavy metal oxide glasses like PbO, Bi_2O_3, Fe_2O_3, MoO_3, Ga_2O_3 and TeO_2 glasses exhibit lower photon energy, high refractive index [**6-10**]. These glasses are more transparent, favorable substance for instruments of optics, optoelectronics, optical instruments, sensors, mechanical, thermal and chemically stable, also provide electrical and superior optical characters [**10**].

Glasses based on tellurite composition examined as favorable substance for their clearness in a wide wavelength, low melting point, more durability as chemical nature, wide IR transmittance, low phonon energy and non-hygroscopic behavior with more linear refractive index. The most significant aspect is that the formation of glass by TeO_2 is occurred only by adding any suitable glass forming and intermediate glass oxide [**11-13**]. The forming ability of glass system, enhancement of thermal stability, optical features of obtained glass would be achieved by mixing of B_2O_3 with TeO_2. The outcome of boro-tellurite composition glass has wide applications in several areas such as storage capacity of optical data, sensors of pressors, optical modulators and also used for hosts of new laser material in radiation protecting shields and optical amplifiers [**14,15**]. TeO_2 belongs to a intermediate glass forming oxide, which does not form glass substance by themselves by adding some additives like lithium, barium, cadmium and zinc oxides [**16**]. The essential changes were taken place by adding of alkali, alkaline earth oxides on the structural and physical features of tellurite glasses have been reported [**17, 18**]. The following tellurite-based glasses with different glass systems like ZnO-TeO_2, Li_2O-TeO_2, TeO_2-CdO and ZnO-CdO-TeO_2 [**19-26**] were prepared and discussed various physical, optical and thermal properties. The formation of TeO_2 glass is like a paratellurite of unlimited three-dimensional network chains of Te-O-Te linkages are formed due to TeO_4 trigonal bipyramids. The addition of some oxides like Li_2O, ZnO and CdO to TeO_2 break the unlimited Te-O-Te network chains there by regular changing structural units of TeO_4 to TeO_3. By adding the above said oxides to TeO_2, the glass system is formed and improve the thermal stability. Here ZnO acts as intermediate glass former and Li_2O served as glass modifier. Hence, we proposed to investigate various optical and structural features by the require mol% of Li_2O with ZnO content on CdO-TeO_2 glass composition.

[1]Department of Physics, Osmania University, Hyderabad 500007, India
[2]Department of Physics, Palamuru University, Mahabubnagar 509001, India

*Corresponding author:
E-mail: praveenaou@gmail.com (K.P.) prasad5336@yahoo.co.in (M.P.)

DOI: 10.5185/amlett.2022.021695

Preparation method

Composition of glass preparation

The glasses were made with chemical mixture of TeO_2 (99+% purity), ZnO (99+% purity), CdO (99+% purity), Li_2O (99.9% purity) and V_2O_5 (99.9% purity) by melt quenching method with required quantity. The powder mixture was mixed carefully and then transferred to porcelain crucibles. The crucible was placed in a high temperature electrical furnace and covered with a lid and heated up to 450 °C/ 30 min to avoid the instability of the compound or impurities and depending on the glass composition the temperature of furnace was raised up to 850-900 °C. The glass sample is rapidly transferred into another steel plate which is retained at 200 °C and quenched with another steel plate maintained at the same temperature. The prepared glasses were allowed to anneal at 200 °C/12 h to take out thermal strains. The processed samples were free from bubble, transparent and non-hygroscopic in nature. Five glass samples with different chemical composition of TCZL series were prepared by changing the mol% of ZnO and Li_2O contents. The obtained glass samples with varying *x* values were mentioned below along with their codes.

TCZL 1:64TeO_2-15CdO- 20ZnO -1V_2O_5,
TCZL 2:64TeO_2-15CdO -15ZnO -5Li_2O -1V_2O_5,
TCZL 3:64TeO_2-15CdO -10ZnO -10Li_2O -1V_2O_5,
TCZL 4:64TeO_2-15CdO -5ZnO -15Li_2O -1V_2O_5,
TCZL 5:64TeO_2-15CdO -20Li_2O -1V_2O_5

Characterization

The X-ray diffraction analysis is a basic identification for amorphous behavior of processed glass samples were carried out by using copper target (K_α= 1.54 Å) at room temperature on Philips PW (1140) diffractometer. By avail of principle of Archimedes and a sensitive balance and xylene (ρ_x = 0.865 g/cc) was used for measured of values as an immersion liquid. The compositional analysis of all the glass samples were also performed by Energy Dispersive Analysis of X-rays (EDAX) method using Carl-Zeiss Ultra 55 model. The FTIR spectra of glass samples were obtained at room temperature using Perkin-Elmer spectrometer model 1605 using KBr disc technique in the range 400-1200 cm^{-1}. The processed sample were grounded to fine particles and then mixed with KBr in the ratio of 0.002:0.2 g. The weighed mixture was then subjected to pressure of 5 tons/cm^2 and the spectra of transmission were recorded soon after making the required disks. Differential scanning calorimetry (DSC) is employed to study the internal changes in TCZL glass structure. The glass transition temperature (T_g) was recorded using a TA instrument 2910 with the temperature range up to 500 °C. All the glass samples were heated at a rate of 10 °C/min in aluminum pans. The UV spectra of the sample of glass material were obtained by using a double beam Schimadzu UV-Vis-NIR-3100 spectrophotometer instrument in the wavelength range 250 - 800 nm at room temperature.

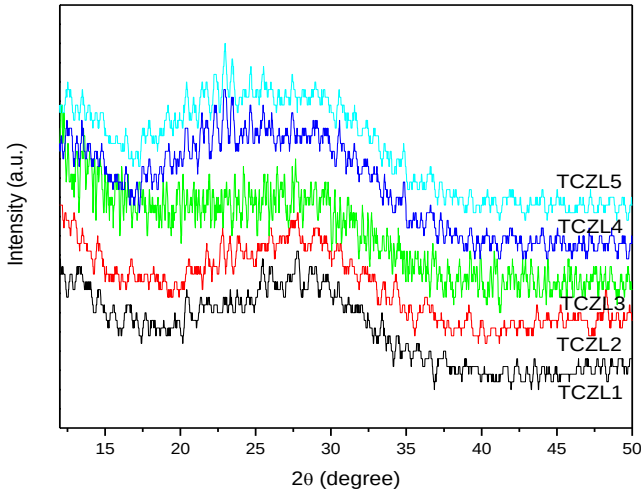

Fig. 1. XRD patterns of TCZL glass system.

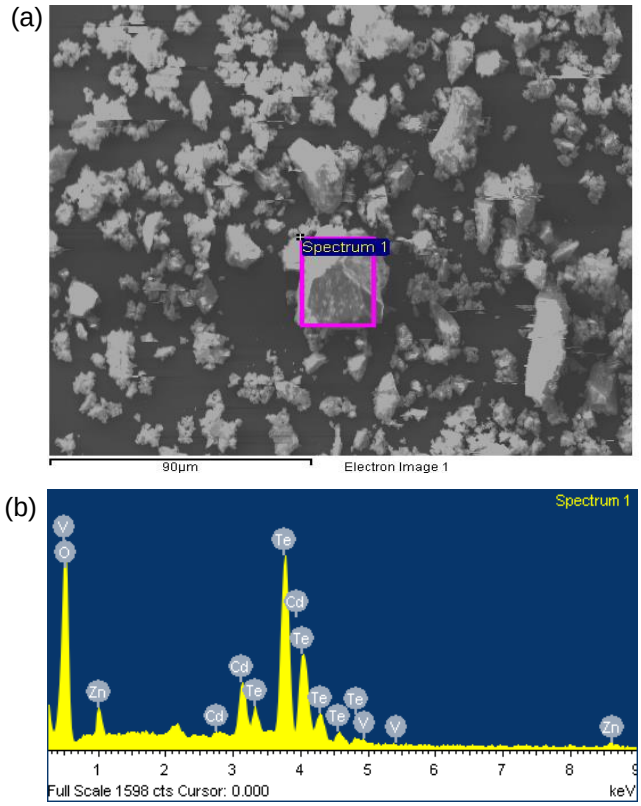

Fig. 2. (a) SEM picture of TCZL3 glass sample. (b) Microstructure of TCZL3 glass sample.

Results and analysis

X-ray diffraction and physical properties

Fig. 1 represents the X-ray diffraction (XRD) patterns of five glass samples of TCZL glass system. The XRD patterns revels the non-crystalline in nature as there are no observable sharp and intense peaks and the **Fig. 2 (a & b)** represents the SEM and EDAX of TCZL with 1 mol% of V_2O_5 glass sample. In addition, it conforms that the component ions are present in the glass sample.

The solidity of all glass samples was observed by using Archimedes principle

$$\rho = \frac{a}{a-b} \times \rho_x \quad (1)$$

Here in the above equation 'a' is the weight of the prepared glass sample in air, 'b' is the weight of the prepared glass sample when immersed in xylene and ρ_x is the density of xylene (0.865 g/cc). The density is an important physical parameter of the glass to detect the internal changes in the formation of glass network like coordination number, geometrical configuration, cross liked density etc. [**27**]. From the calculated density values, we calculated the molar volume (V_m) of the glass samples using the below mentioned equation.

$$\text{Molar volume } V_m = \frac{M}{\rho} \quad (2)$$

where, M is the molecular weight of each sample and ρ is the density of each glass sample.

Oxygen packing density (OPD) of each glass sample was measured from the density using the below formula. By using this formula one can determined the number non bridging oxygens.

$$\text{Oxygen Packing Density (OPD)} = \frac{\rho}{M} \times O_n \quad (3)$$

O_n = the number of oxygen atoms in glass sample formula.

The decrease in densities at room temperature from 5.629 to 5.053 results in increase of molar volume of the glass sample from 24.780 to 27.309. Oxygen packing density (OPD) values decreases (67.794 to 61.516). The Molar volume (V_m) and oxygen packing density (OPD) values are measured and presented in **Table 1**. Hence, it is clear that substitution of Li_2O in place of ZnO content since lower molecular weight of Li_2O results in increase of molar volume and also larger values of radial bond length of Li-O to Zn-O variation in OPD values. The decrease in OPD values with decrease in ZnO content and increases with Li_2O at constant [$64TeO_2$-15CdO] showing the formation of TeO_4 and ZnO_4 units resulting the enhancement in number of non-bridging oxygen (NBO).

Table 1. Physical parameters of TCZL glass system.

Sample Code	Density ρ (g/cc)	Molar Volume Vm (cc/mol)	Oxygen Packing Density (O.P.D) (mol/l)	Optical basicity (Λ)
TCZL 1	5.629	24.780	67.794	0.998
TCZL 2	5.449	25.528	65.809	0.978
TCZL 3	5.329	26.036	64.526	0.967
TZCL 4	5.208	26.564	63.241	0.957
TCZL 5	5.053	27.309	61.516	0.946

FTIR

The FTIR transmittance spectrum of VO^{2+} doped TCZL glass samples were shown in **Fig. 3** and the position of transmitted bands and vibrational modes were listed in **Table 2** and **Table 3**. The transmittance bands appeared in the range of 441-452 cm^{-1} were assigned to the symmetrical stretching or bending vibrations of ZnO_4 tetrahedral linkages which are produced due to the Zn-O bonds [**28, 29**]. This band shifts from lower to higher with the increase of Li_2O and decrease of ZnO content. Hence, it is evident that the low intensity bands appeared in the range of 441-452 cm^{-1}. The bands observed in the range 676-681 cm^{-1} are due to axial symmetrical stretching vibrational modes of tetrahedral Te_{eq}-O-Te_{eq} of TeO_4 and the Te-O-Te, O-Te-O equatorial symmetrical, asymmetrical stretching vibrational modes of TeO_{3+1} trigonal bipyramidal or TeO_3 trigonal pyramidal units. This transmitted bands shifts from low wavenumber to high wavenumber due to internal structural modifications in the prepared glass system. This explains that the addition of ZnO could break the axial Te-O bonds of TeO_4 units, resulting in progressive changes in the coordination of Te^{+4} ions and also suggests an increase of lower coordination units TeO_3 as compared to higher coordination units TeO_4. These bands are probably due to distribution of bond-angle, bond radius and variation of the local electronic atomic environment in the amorphous state [**30**]. The bands observed in the range of 764-771 cm^{-1} shows the corner sharing of Te-O-Te linkages. This could suggest that the glass network may form Zn-O-Te / Te-O-Zn bonds in place of Te-O-Te linkages. The band observed in the range of 906-910 cm^{-1} is assigned to the stretching vibrations of Te-NBO with the addition of Li_2O and ZnO contents. In the present glass matrix, the above four regions of bands observed by addition of Zn^{2+} introduces coordination defects by breaking the linkages of Te-O-Te/Te-O-Zn or Te-O-Cd. From the above changes of the IR spectral studies, the following assumptions were made: (i) pure TeO_2 was not observed so trigonal bipyramidal [TeO_4] structural units were transformed into trigonal pyramidal [TeO_3]. (ii) The 840 cm^{-1} absorption band was not noticed in these FTIR spectra suggest that formation of tetrahedral coordination of CdO_4 is not seen. (iii) The concentration of ZnO up to 20 mol% acts as a network modifier so that increases the non-bridging oxygen molecules in glass network.

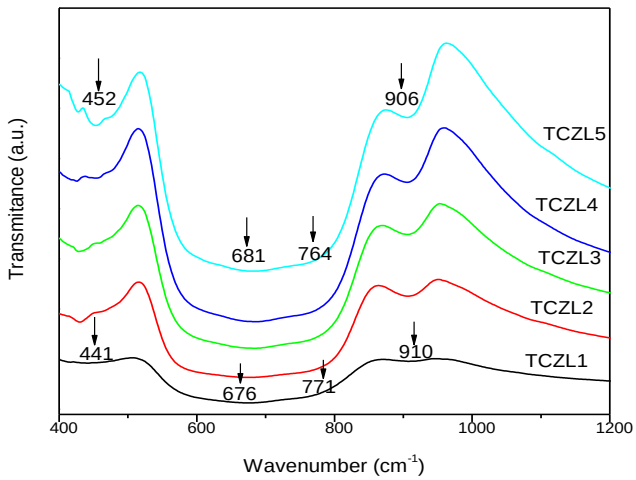

Fig. 3. FTIR spectra of TCZL glass system.

Table 2. FTIR band position of TCZL glass system.

Sample Code	Band position(cm^{-1})			
TCZL 1	441	676	771	910
TCZL 2	430	675	765	908
TCZL 3	429	679	758	907
TCZL 4	446	680	760	908
TCZL 5	452	681	764	906

Table 3. FTIR band assignments of TCZL glass system.

Wavenumber (cm^{-1})	Assignments
441-452	Vibrations of CdO and ZnO tetrahedral
675-681	Stretching vibrations of Te-O bonds in TeO_3 and TeO_4 groups
758-771	Vibrations of Te-O-Te / Te-O-Zn bonds which suggests the formation of TeO_4 units and at the expense of TeO_3 units
906-910	Stretching vibrations of Te-NBO / metal-NBO vibrations

Table 4. DSC Parameters of TCZL glass system.

Sample code	Tg (ºC)	To (ºC)	Tp (ºC)	ΔT = To– Tg (ºC)
TCZL 1	325	420	438	95
TCZL 2	273	---	---	---
TCZL 3	261	336	353	75
TCZL 4	247	310	336	62
TCZL 5	227	288	297	61

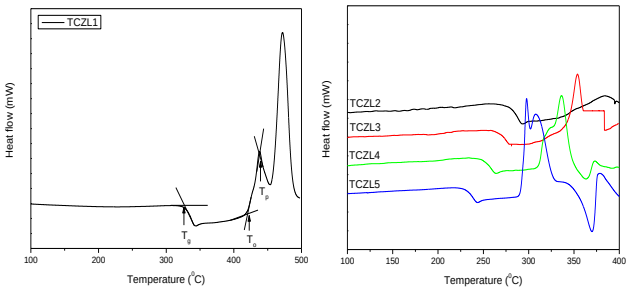

Fig. 4. DSC thermograms of TCZL glass system.

Differential scanning calorimetry

From **Fig. 4**, the DSC thermogram shows multiple crystallization peaks, which explains that the glass samples contain different crystalline phases. The analysis of the samples shows similar conclusions from the DSC thermograms and determined the glass transition temperature (T_g), the onset crystalline temperature (T_o) and peak crystalline temperature (T_p) as presented in **Fig. 4** and values are mentioned in **Table 4**. By changing the x affects structural modifications, which are due to T_g and it is very sensitive to any change of the coordination number of the network-forming atoms and also to the formation of non-bridging oxygens. The glass transformation does not take place at a defined temperature, but within a temperature range, representing the transformation region, the glass transition temperature (T_g) depends on the character of the substance studied and on the thermal history of the sample. The **Fig. 4** shows decreasing in T_g from 325 to 227 °C with an increase of Li_2O content from 0 to 20 mol%, which indicates a reduction in the rigidity of the glass network. This result indicates the argument of cross-linked density of various microstructural groups and closeness of their packing with decreasing of density and molar volume increasing by the addition of Li_2O content. The $\Delta T=(T_o-T_g)$ measures the thermal stability of super cooled glass is directly proportional to the glass strength.

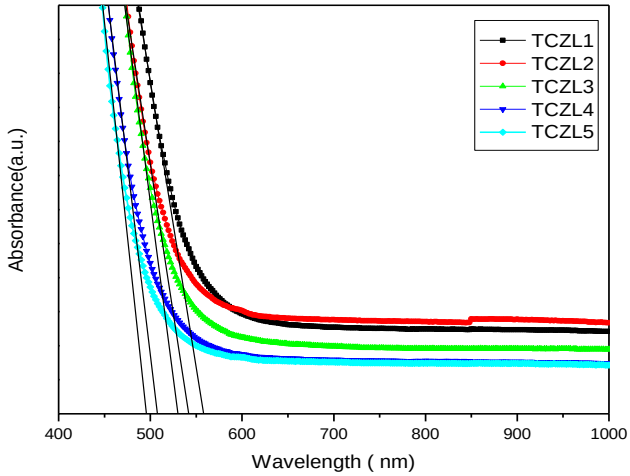

Fig. 5. Optical absorption spectra of TCZL glass system.

Optical studies

Optical basicity (Λ_{th}) is calculated by Duffy and Ingram [**31, 32**] suggested to the individual oxides that is,

$$\Lambda_{th}=x(TeO_2)\Lambda(TeO_2)+x(ZnO)\Lambda(ZnO)+x(CdO)\Lambda(CdO)+x(Li_2O)\Lambda(Li_2O)+x(V_2O_5)\Lambda(V_2O_5) \quad (4)$$

where $x(TeO_2)$, $x(ZnO)$, $x(CdO)$, $x(Li_2O)$, and $x(V_2O_5)$ are the equivalent mole fractions of different oxides and Λ (TeO_2=0.93), Λ (CdO=1.115), Λ (ZnO=1.08), $\Lambda(Li_2O$=0.87) and $\Lambda(V_2O_5$=1.04) are optical basicity values [**33**]. The calculated values of optical basicity changed from 0.988 to 0.946 and noticed that basicity decreases with decrease in ZnO and increase in Li_2O content. Therefore, replacement of higher basicity by lower basicity has resulted as decrease in theoretical optical basicity. Optical absorption spectra of present TCZL glass system have been plotted and shown in **Fig. 5**. The wavelengths subjected to absorption edge are taken as cut off wavelengths where the intensity move the optimum value in absorption of spectra as presented in **Fig. 5** and the values are noted in the **Table 5**. From these we found that the basic absorption edge was shifted to lower wavelength side as Li_2O content is elevated from 0 to 20 mol%. The lowest cut off wavelength or highest band gap observed in 0 mol% of Li_2O glass system is due to the formation of TeO_4 units that are changed with ZnO and CdO units. In the near absorption edge, absorption coefficient of the glass sample of thickness 't' can be calculated using the following relation [**34**].

$$\alpha(\omega) = \left({}^{1}/_{t}\right) \ln \left({}^{I_o}/_{I}\right) \quad (5)$$

The equation between absorption coefficient $\alpha(\omega)$ and phonon energy $(h\upsilon)$ of incident radiation is given by the relation [**35**]. For indirect transition that is for non-crystalline materials the above relation can be written as

$$(\alpha h\nu)^{1/2} = B(h\nu - E_{opt}) \quad (6)$$

using above relation E_{opt} values are determined by extrapolation of linear region of the plots of $(\alpha h\nu)^{1/2}$ against hν to $(\alpha h\nu)^{1/2} = 0$ as shown in **Fig. 6** and the values of E_{opt} thus obtained for all glass samples are given in **Table 5**. The optical energy gap increases with an increase of Li_2O (decreases of ZnO mol%) content, which creating a breakdown of continuous glass network reflected in the absorption spectra by a noticeable moving of absorption edge to lower wavelength side which is due to structural rearrangements of relative concentrations of various fundamental units due to the migrating of absorption band to lower energy represents to the transition from the non-bridging oxygen that binds an electron more loosely than bridging oxygen. Band tailing parameter (p) gives the information about indirect allowed transitions is measured from the slope of curve $(\alpha h\nu)^{1/2}$ against hν.

Refractive index (n) is measured from the optical energy gap using the relation given by Dimitrov and Sakka [**36**] and given as

$$\frac{n^2-1}{n^2+2} = 1 - \sqrt{\frac{E_{opt}}{20}} \quad (7)$$

from which it is clear that refractive index values decline with increase of E_{opt} values with varying Li_2O and ZnO contents. The refractive index values from 2.638 to 2.528, which may be due to increase in iconicity of Li^+ ions and the decline in optical basicity. Natural logarithm of absorption coefficients $\ln(\alpha)$ is plotted against photon energy $(h\upsilon)$ is plotted by Urbach plots for tested glass system and it is shown in **Fig. 7**. The values of Urbach energy are measured from the slopes of the linear region of the curves at low phonon energies and taking their reciprocals and is found that Urbach energy increases with an increase of Li_2O due to increase in fragile nature of the glass network [**37**]. In the present glass system the values of Urbach energy lie between 0.886 to 0.651 eV and the higher Urbach energies indicates glass system of high defective nature. The density of a glass plays a vital role in maintaining the refractive index [**38**]. In many cases, the decline in the refractive index is followed by the decline in density [**39**].

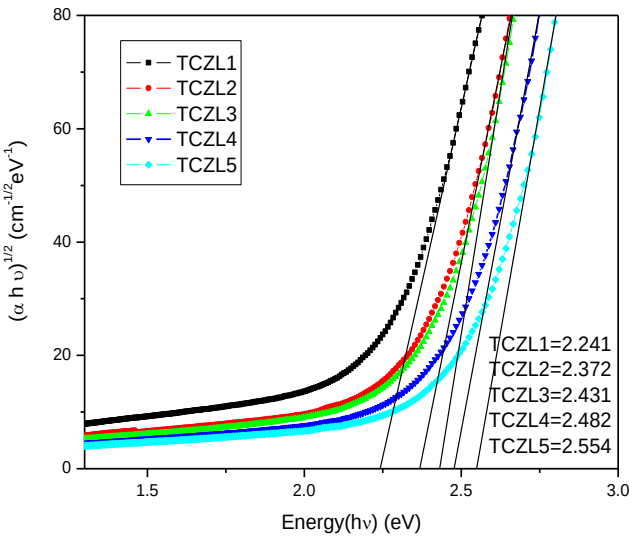

Fig. 6. Tauc's plots of TCZL glass system.

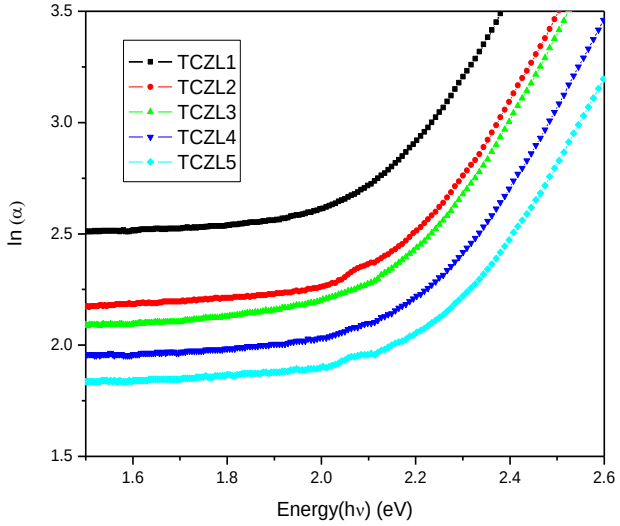

Fig. 7. Urbach plot of TCZL glass system.

Table 5. Optical parameters of TCZL glass system.

Sample code	Cut Off Wave Length (nm)	Optical Energy gap Eopt (eV)	Urbach Energy E (eV)	Band Tailing Parameter (P) (cm eV)	Refractive Index (n)	Molar Refractivity (Rm)	Metallizatin Parameter (M)
TCZL 1	557	2.241	0.886	69.909	2.638	16.485	0.334
TCZL 2	540	2.372	0.651	85.902	2.590	16.736	0.334
TCZL 3	528	2.431	0.245	86.686	2.569	16.958	0.348
TCZL 4	506	2.482	0.620	93.368	2.552	17.206	0.352
TCZL 5	494	2.554	0.632	76.900	2.528	17.550	0.357

From the refractive index we find the molar refractivity (R_m) is directly proportional to the polarizabilities of the constituent ions of the glass. The molar refractivity indicates the role of ionic packing in maintaining the refractive index of a glass. The R_m is given by the expression

$$R_m = V_m \left[\frac{n^2-1}{n^2+2}\right] \quad (8)$$

where, V_m is the molar volume of the glass and is the refractive index at the wavelength of measurement. The molar refractivity increases from 16.485 to 17.550 with increasing of Li_2O content. The metallization criterion is predicting that the glass samples are shows metallic insulating behavior [40] and it is given by the following expression.

$$M = 1 - R_m/V_m \quad (9)$$

The calculated metallization parameter (M) values show less than one it behaves like a insulating nature or greater than one it behaves like a insulating nature. Therefore, the present glasses samples shows increased tendency for metallization and the values are presented in **Table 5**.

Conclusions

The $64TeO_2$-15CdO-(20-x)ZnO-xLi_2O-$1V_2O_5$ glass system have been successfully synthesized by melt quenching method. The XRD spectra authenticated the non-crystalline nature of the fabricated glasses. FTIR studies have shown that the adding of Li_2O in place of ZnO elevation of number of non-bridging oxygen by gradually replacing trigonal bipyramids TeO_4 units with trigonal pyramids TeO_3 through TeO_{3+1}. DSC confirms the non-crystalline nature of the prepared glasses. The increase of Li_2O content results in the elevation of optical band gap (E_{opt}) from 2.241 to 2.554 eV, molar refractivity (R_m) values increased from 16.485 to 17.550, metallization parameter of the present glass system shows increasing tendency of metallic nature and the refractive index (n) decreased from 2.638 to 2.528. The introduction of Zn^{2+} breaks Te-O bonds in the TeO_2 network, creating non-bridging oxygen molecules. The calculated values of Urbach energy were in the range of 0.886 to 0.651 eV and these values signify them order and disordered state of glasses. The optical basicity values are observed to be in range 0.998 to 0.946 for the present glass system. The density of VO^{2+} doped lithium zinc cadmium tellurite glasses declined from 5.629 to 5.053 g/cc with the addition of Li_2O. The decrease of T_g from 325 to 227 °C indicates decrease in the cross-linking network density, in spite of the development of TeO_3 units and smaller thermal stability (ΔT). Hence, present investigated glasses are promising for the potential ese in shielding applications.

***Scientific words/Names/Formulas/Measurements/Methods are listed below:**

$64TeO_2$-15CdO-(20-x) ZnO-xLi_2O-$1V_2O_5$
X- ray diffraction
density (ρ)
molar volume (V_m)
oxygen packing density (OPD)
refractive index (n)
molar refractivity (R_m)
metallization parameter (M)
Optical basicity (Λ_{th})
Fourier transform infrared spectroscopy (FTIR)
Differential scanning calorimetry (DSC)
glass transition temperature (T_g)
thermal stability ($\Delta \boldsymbol{T}$)
cut-off wavelength (λ)
optical energy gap (E_{opt})
Urbach energy ($\Delta \boldsymbol{E}$)
ZnO, CdO, CdO_4, Li_2O, TeO_2, TeO_3, TeO_4, Te-O-Te, Te-O-Zn and Te-O-Cd
Instrument names, Scientists and Reference authors names.

Keywords

XRD, SEM, Optical absorption, DSC, FTIR, Glass transition temperature.

References

1. Kurtulus, R.; Kavas, T.; *Phys. Chem.*, **2020**, *176*, 109090. https://doi.org/10.1016/j.radphyschem.2020.109090
2. Rüssel, C.; Introduction to Glass Science and Technology, **1999**, 208.
3. Al Buriahi, MS.; Hegazy, HH.; lresheedi, FA.; Olarinoye, IO.; Algarni, H.; Tekin, HO.; Saudi, HA. Ceramics International, **2021**, 47, 5951. https://doi.org/10.1016/j.ceramint.2020.10.168
4. Shaaban, KS.; Wahab, EAA.; Shaaban, ER.; Yousef, ES.; Mahmoud, SA.; *Opt. Quant Electron*, **2020**, 52, 125. https://doi.org/10.1007/s11082-020-2191-3
5. Shaaban, K.; Abdel Wahab, EA.; El-Maaref, AA.; Abdelawwad, M.; Shaaban, ER.; El Sayed, Y.; Wilke, H.; Hillmer, H.; Börcsök, J.; *J. Mater. Sci. Mater. Electron*, **2020**, 31, 4986. https://doi.org/10.1007/s10854-020-03065-8
6. Ersundu, A.E.; Çelikbilek Ersundu, M.; Gedikoğlu, N.; *J. Non-Cryst Solids*, **2020**, *541*, 120093. https://doi.org/10.1016/j.jnoncrysol.2020.120093
7. Abd-Allah, WM.; Saudi, HA.; Shaaban, KS.; Farroh, HA.; *Appl. Phys. A Mater. Sci. Process*, **2019**, *125*, 275. https://doi.org/10.1007/s00339-019-2574-0
8. El-Sharkawy, RM.; Shaaban, KS.; Elsaman, R.; Allam, EA.; El-Taher, A.; Mahmoud, ME.; *J. Non-Cryst Solids*, **2020**, 528, 119754. https://doi.org/10.1016/j.jnoncrysol.2020
9. Shaaban, KS.; Koubisy, MSI.; Zahran, HY.; Yahia, IS.; *J. Inorg Organomet Polym.*, **2020**, 30, 4999. https://doi.org/10.1007/s10904-020-01640-4
10. Dumbaugh, WH.; Lapp, JC.; *J. Am. Ceram Soc.*, **1992**, 75, 2315. https://doi.org/10.1111/j.1151-2916.1992.tb05581.x
11. Yongtao, Z.; Yunxia, Y.; Feihong, H.; Jing, R.; Shuanglong; Guorong, Ch.; *J. Non-Cryst. Solids*, **2014**, 386, 90. https://doi.org/10.1016/j.jnoncrysol.2013.11.037
12. Guoying, Z.; Ying, T.; Huiyan, F.; Junjie, Z.; Hu, L.; *J. Mater. Sci. Technol.* **2013**, *29*, 209. https://doi.org/10.1016/j.jmst.2012.11.003
13. Sayyed, MI.; Al-Hadeethi, Y.; Maha AlShammari, M.; Ahmed, M.; Saleh Al-Heniti, H.; Rammah, YS.; *Cera. Inter.*, **2021**, *47*, 611. https://doi.org/10.1016/j.ceramint.2020.08.168
14. Hegazy, HH.; Al-Buriahi, MS.; Alresheedi, F.; Alraddadi, S.; Arslan, H.; Algarni, H.; *J. Inorg. Organometallic Poly. Mater.*, **2021**, *31*, 2331. https://doi.org/10.1007/s10904-021-01933-2
15. Taher, AE.; Ali, AM.; Saddeek, YB.; Elsaman, R.; Algarni, H.; Shaaban, K.; Amer, TZ.; *Radiat. Phys. Chem.*, **2019**, *165*, 108403. DOI: https://doi.org/10.1016/j.radphyschem.2019.108403

16. Sarjeant, P; Roy, R.; *J. Am. Cer. Soc.*, **1967**, *50*, 500. DOI: 10.1111/j.1151-2916.1967.tb14980.x
17. Sekiya, T.; Mochida, N.; Ohtsuka, A.; *J. Non-Cryst. Solids*, **1994**, *168*, 106. DOI: 10.1016/0022-3093(94)90125-2
18. Sekiya, T.; Mochida, N.; Ohtsuka, A.; *J. Non-Cryst. Solids*, **1992**, *144*, 128. DOI: 10.1016/S0022-3093(05)80393-X
19. Lei, N.; Xu, B.; Jiang, Z.; *Opt. Commun.*, **1996**, *127*, 263. DOI: 10.1016/0030-4018(96)00099-5
20. Rolli, R.; Gatterer, K.; Wachtler, M.; Bettinelli, M.; Speghini, A.; D. Ajo, D.; *Spectrochem. Acta Part A.*, **2001**, *57*, 2009. DOI: 10.1016/S1386-1425(01)00474-7
21. Iparraguiree, I.; Azkargorta, J.; Fernadez-Navarro, J.M.; Al-Saleh, M.; Fernandez, J.; Balda, R.; *J. Non-Cryst. Solids.*, **2007**, *353*, 990. DOI: 10.1016/j.jnoncrysol.2006.12.103
22. K. Upendra Kumar, K.; Prathysha, V.A.; Babu, P.; Jayasankar, C.K.; Joshi, A.S.; Speghini, A.; Bettinelli, M.; *Spectrochim. Acta A.*, **2007**, *67*, 702. DOI: 10.1016/j.saa.2006.08.027
23. Babu, S.S.; Rajeswari, R.; Jang, K.; Jin, C.E.; Jang, K.H.; Seo, H.J.; Jayasankar, C.K.; *J. Lumin.*, **2010**, *130*, 1021. DOI: 10.1016/j.jlumin.2010.01.017
24. Araujo, E.B.; Idalgo, E.; *Opt. Mater.*, **2011**, *33*, 1847. DOI: 10.1016/j.optmat.2011.02.044
25. Karaduman, G.; Ersundu, A.E.; Celibilek, M.; Solak, N.; Aydin, S.; *J. Eur. Cer. Sci.*, **2112**, *32*, 603. DOI: 10.1016/j.jeurceramsoc.2011.09.027
26. Ruvalcaba-Cornejo, C.; Zayas, Ma.E.; Castillo, S.J.; Lozada Morales, R.; Perez-Tello, M.; Diaz, C.G.; Rincon, J. Ma.; *Opt. Mater.*, **2011**, *33*, 823. DOI: 10.1016/j.optmat.2011.01.001
27. El-Egili, K.; Oraby, A.; *J. Phys. Condens. Matter.*, **1996**, *8*, 8959. DOI: 10.1088/0953-8984/8/46/003/pdf
28. Tarte, P.; *Bull. Soc. France Ceram.*, **1963**, *58*, 13.
29. Tarte, P.; *Silic. Ind.*, **1963**, *28*, 345.
30. Shaltout, I.; Yi Tang.; Braunstein, R.; Shaisha, E.E.; *J. Phys. Chem. Solids*, **1996**, *57*, 1223. DOI: 10.1016/0022-3697(95)00309-6
31. Duffy, J.; Ingram, M.; *J. Non-Cryst. Solids.*, **1976**, *21*, 373. DOI: 10.1016/0022-3093(76)90027-2
32. Duffy, J.; Ingram, M.; *J. Am. Chem. Soc.*, **1971**, *93*, 6448. DOI: 10.1021/ja00753a019
33. Dimitrov, V.; Komatsu, T.; *J. Solid State Chem.*, **2002**, *163*, 100. DOI: 10.1006/jssc.2001.9378
34. Sands, R.H.; *Phys. Rev.*, **1995**, *99*, 1222. DOI: 10.1103/PhysRev.99.1222
35. Daavis, E.A.; Mott, N.F.; *Phil. Mag.*, **1970**, *22*, 903. DOI: books?id=Pl1b_yhKH-YC (Book)
36. Dimitrov, V.; Sakka, S.; *J. Appl. Phys.*, **1996**, *79*, 1736. DOI: 10.1063/1.360962
37. Gayathri Pavani, P.; Suresh, S.; Chandra Mouli, V.; *Opt. Mater.*, **2011**, *34*, 215. DOI: 10.1016/j.optmat.2011.08.016
38. Shelby, J.E., Introduction to glass science and technology (2nd edition). United Kingdom: Cambridge: The Royal Science of Chemistry, **2005**. DOI: 10.1039/9781847551160
39. Fanderlik, I.; Glass Science and technology: Optical properties of glasses. Amsterdam: Elsevier Science Publisher, **1983**. DOI: https://www.worldcat.org/title/optical-properties-of-glass/oclc/9643524
40. Sreenivasulu, V.; Upender, G.; Swapna.; Vamsi Priya, V.; Chandra Mouli, V.; Prasad, M.; *Physica B.*, **2014**, *454*, 60. DOI: 10.1016/j.physb.2014.06.039